

Thermally induced dimensional crossover in single-crystal $\text{Bi}_2\text{Sr}_2\text{CaCu}_2\text{O}_x$

Yoichi Ando* and Seiki Komiya

Central Research Institute of Electric Power Industry, 2-11-1 Iwato-kita, Komae, Tokyo 201, Japan

Yasutoshi Kotaka and Kohji Kishio

Department of Applied Chemistry, University of Tokyo, Hongo, Bunkyo-ku, Tokyo 113, Japan

(Received 5 April 1995)

The linear ac magnetic response of three $\text{Bi}_2\text{Sr}_2\text{CaCu}_2\text{O}_x$ single crystals with various doping states was investigated with a miniature two-coil mutual inductance technique in magnetic fields parallel to the c axis. The dissipation peak appeared right below T_c , and a drop in dissipation was observed at a frequency-independent temperature T_D together with an increase in shielding signal, upon field cooling the sample. The observed frequency-independent feature can be understood as a consequence of the thermally induced dimensional crossover.

The electronic and magnetic properties of $\text{Bi}_2\text{Sr}_2\text{CaCu}_2\text{O}_x$ in the superconducting state have proved to be rich in new physics because of its large anisotropy. One of the subjects still needing to be clarified is the dimensional crossover in the vortex system with the magnetic field parallel to the c axis. There are theoretical suggestions¹⁻³ that thermal fluctuations of the pancake vortices⁴ lead to a thermally induced dimensional crossover, above which the superconducting layers are effectively decoupled and behave as a two-dimensional (2D) system. It has been predicted¹⁻³ that changes in the c -axis transport and/or the tilt elastic modulus C_{44} should occur at this thermally induced crossover. Recent development of the Ginzburg-Landau (GL) fluctuation theory in terms of the Landau-level representation also predicts a similar dimensional crossover.⁵ Several experiments have been done on this subject with transport measurements,^{3,6,7} however, the conclusions are diverse.

We note that a crossover of different origin, a *magnetically* induced dimensional crossover, has been reported in some experiments on $\text{Bi}_2\text{Sr}_2\text{CaCu}_2\text{O}_x$ single crystals, such as small angle neutron scattering,⁸ μSR ,⁹ irreversibility line,^{10,11} and magnetization.¹² If the pinning in each layer is sufficiently strong, the correlation between pancake vortices in the c direction is considerably destroyed above a crossover field B_{2D} , because the magnetic interaction between pancakes in the same layer becomes stronger than that between pancakes in adjacent layers^{8,13} and the positions of the pancakes are optimized within each layer. In this sense, we call it a magnetically induced crossover. B_{2D} has been reported to be around 50 mT (Refs. 8-12) and temperature independent.⁸

In this paper, we report the *thermally* induced dimensional crossover observed in the linear ac magnetic response of high-quality $\text{Bi}_2\text{Sr}_2\text{CaCu}_2\text{O}_x$ single crystals in dc fields parallel to the c axis. We measured three single crystals, underdoped ($T_c = 87$ K), optimally doped ($T_c = 92$ K), and overdoped ($T_c = 75$ K) crystals, which were carefully heat treated to control the anisotropy by changing the carrier doping.^{12,14} A miniature two-coil mutual inductance technique^{15,16} was used in this work, where a small (≈ 0.6 mm diameter) coaxial set of

pickup/drive coils was placed on the center of the top ab face of a crystal (see the inset of Fig. 1). Details of our two-coil measurements have been described elsewhere.¹⁶ The primary difference between our technique and other ac-magnetic measurements is that our technique is sensitive to the shielding current flowing near the center of the sample, while others are mostly sensitive to currents near the edges.

The crystals were grown by the floating-zone method. Details of the heat treatment of the as-grown crystals have been described elsewhere.^{12,14} The ab faces of all the crystals measured were larger than 2.5×3 mm². Since the diameter of our two-coil probe is about 0.6 mm, the lateral dimensions of the samples are more than four times larger than the coil size. The thicknesses of the crystals were 74, 60, and 70 μm for the underdoped, optimally doped, and the overdoped crystals, respectively. These crystals were taken from a single as-grown rod; therefore, the compositions of the crystals are exactly the same except for the oxygen content. The axis of the two-

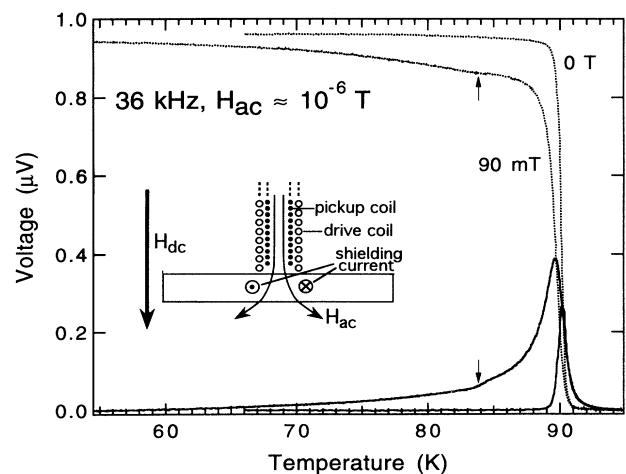


FIG. 1. In-phase (solid lines) and out-of-phase (dotted lines) signals at 36 kHz taken in zero field and 90 mT. The arrows mark the specific feature. Inset: Schematic view of the experiment.

coil probe was parallel to the c axis of the crystals and the dc-magnetic field was applied parallel to these axes. The amplitude of the drive current I_d was 1.25 mA, which produces the ac-magnetic field of about 10^{-6} T at the sample; the linearity of the response with respect to I_d of up to 4 mA was checked for the entire temperature range with all the crystals. All the data were taken in the field-cooled state.

Figure 1 shows the in-phase and out-of-phase signals of the optimally doped crystal in 0 and 90 mT taken at 36 kHz. It can be immediately seen in Fig. 1 that the peak in the in-phase signal at 90 mT appears at an unusually high temperature, 89.7 K. At this temperature, the vortex system is well in the liquid phase, and the vortex diffusion theory^{17–19} should be applicable. The diffusion theory tells us that the dissipation peak appears when the diffusion length (or skin depth) $\delta = (2D/\omega)^{1/2} = [2\rho/(\mu_0\omega)]^{1/2}$ becomes comparable to a relevant sample dimension, where D is the diffusion constant, ω is the angular frequency, and ρ is the resistivity. Since the sample resistivity is still quite large at the peak temperature in 90 mT, the relevant length scale for the dissipation peak should accordingly be large. If we take the distance from the drive-coil edge to the sample edge (≈ 1 mm) for the relevant length scale, ρ is calculated to be $\approx 1 \times 10^{-7}$ Ω m at the peak for 36 kHz. This value is reasonable at the peak temperature in 90 mT.²⁰ Therefore, we can conclude that the diffusion mode associated with the large dissipation peak is the compressive motion of the pancake vortices, which propagates out to the sample edge, caused by the shielding current under the drive coil.

A closer look at the data of 90 mT reveals that there is an additional feature in the response around 84 K (marked by arrows). Below this temperature, the dissipation (in-phase signal) is suppressed and the shielding (out-of-phase signal) is enhanced, suggesting that the vortex system becomes stiffer.¹⁸ To see whether the occurrence of this change is frequency dependent, we took data also at 4, 12, and 110 kHz. The in-phase signals in 90 mT at different frequencies are shown in Fig. 2, where the measured voltage was divided by the drive current and the angular frequency ω to give the inductance change. The inset of Fig. 2 shows the temperature derivative (slope) of the signals normalized by the value at 85 K. It is clear that the temperature where the slope is suddenly enhanced, which we denote T_D , does not depend on ω within the one-and-a-half-decade frequency range, although the large dissipation peak shows a clear shift with frequency. If the feature at T_D is caused by a crossover of the diffusion length with some length scale, the diffusion theory dictates that ρ/ω should have the same value at T_D , which is impossible. Therefore, we can safely believe that the feature at T_D has nothing to do with the so-called “double peak” feature^{19,21} often observed in ac susceptibility measurements and vibrating reed measurements, which is merely the consequence of the two different length scales for the diffusion.

Figures 3(a) and 3(b) show the data of the underdoped and overdoped crystals, respectively, measured at 36 kHz. The qualitative behaviors of these crystals are the

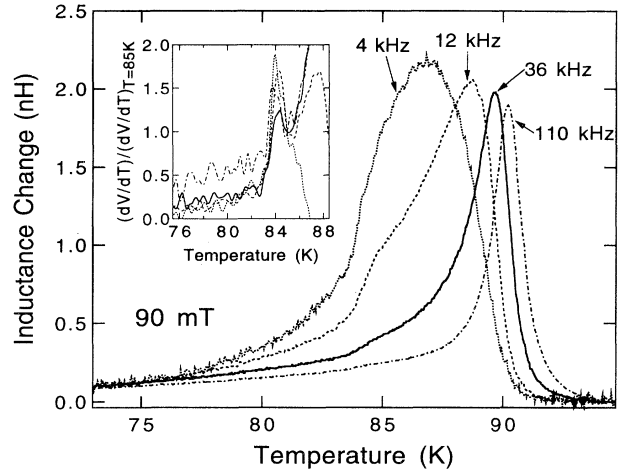


FIG. 2. In-phase signals shown as the inductance change in 90 mT at various frequencies. Inset: Temperature derivative of the signals normalized at 85 K. The line styles of the curves correspond to those in the main panel.

same as that of the optimally doped crystal; namely, the dissipation peaks appear right below T_c , and T_D is well defined. In addition, T_D was frequency independent over one and a half decade also in the underdoped and overdoped crystals. We show, as an example, the data of the underdoped crystal in 10 mT taken at different frequencies, 4, 12, 36, and 110 kHz, in Fig. 4. It is evident that T_D is frequency independent within the accuracy of less than 1 K, although the dissipation peak shows a clear shift in the same frequency range. The insets of Figs. 3(a) and 3(b) are the susceptibility transitions of the overdoped and underdoped crystals, respectively, measured with a Quantum Design superconducting quantum interference device magnetometer in 0.2 mT, which show that both of them are well heat treated and have $\Delta T_c \approx 3$ K. Figure 5 shows the determined $T_D(B)$ lines for these three crystals in the B - T phase diagram, where the temperature was normalized by their T_c . It is obvious that the $T_D(B)$ line moves to lower fields upon increasing the anisotropy (decreasing doping). It should be mentioned that, although not shown here, the irreversibility lines were also measured on these crystals; the $T_D(B)$ lines for the optimum dope and the overdope are far above the irreversibility lines, but the $T_D(B)$ line for the underdope is located very close to the irreversibility line.

Now we discuss the origin of the feature at T_D . One possible interpretation is based on the change in ρ_c at the thermally induced dimensional crossover. We first note that, in the experiments, the axis of the drive coil has a slight misalignment with respect to the c axis of the crystal. This means that the shielding current induced in the sample has some component along the c axis; therefore, the actual resistivity that determines the skin depth may be a mixture of ρ_{ab} and ρ_c . If the local ρ_c (not necessarily the macroscopic ρ_c) begins to increase rapidly around T_D with increasing temperature, the skin depth would also show a noticeable increase, which explains the feature at

T_D in the two-coil response. Such a change in ρ_c has been predicted to occur at the thermally induced dimensional crossover in the Ikeda fluctuation theory.⁵ Also, Daemen *et al.* predicted a vanishing of the c -axis critical current at the crossover. We should mention that another interpretation based on the reduction in C_{44} at the crossover^{1,5} might also be possible. In any case, it is reasonable to analyze our T_D in the light of the thermally induced dimensional crossover. The thermally induced dimensional crossover field $B_D(T)$ predicted by Ikeda's fluctuation theory⁵ is

$$B_D(T) \approx \frac{\Phi_0^3}{4\pi^2 \mu_0 k_B s \gamma^2 \lambda_{ab}(0)^2} \left[\frac{1}{T} - \frac{1}{T_c} \right], \quad (1)$$

where $s = 1.5$ nm is the CuO_2 layer spacing, and $\gamma \equiv \lambda_c / \lambda_{ab}$ is the anisotropy parameter (λ_c and λ_{ab} are the London penetration depths of shielding currents in

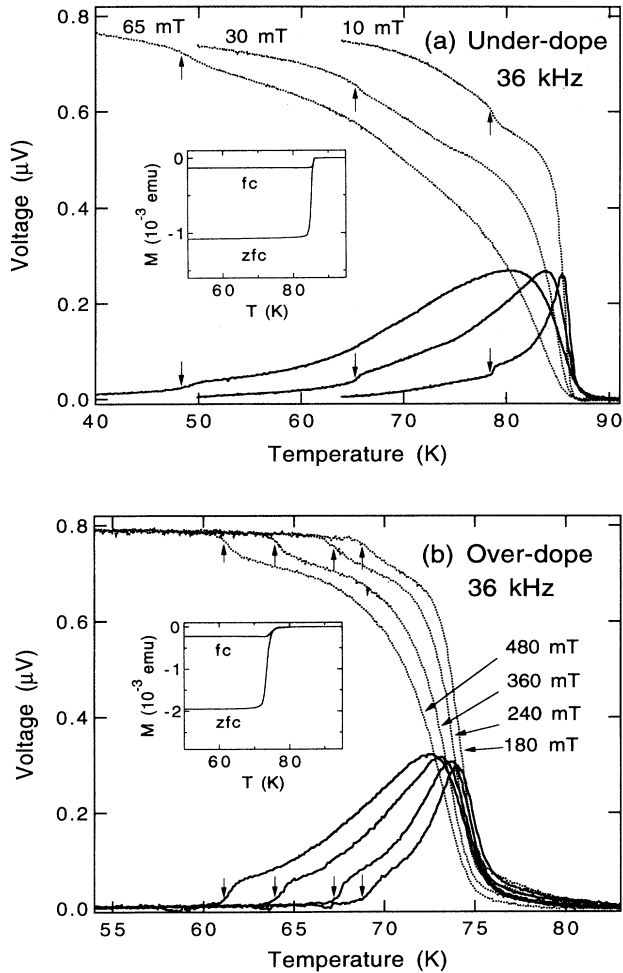


FIG. 3. (a) In-phase (solid lines) and out-of-phase (dotted line) signals of the underdoped crystal measured in 10, 30, and 65 mT at 36 kHz. (b) Signals of the overdoped crystal in 180, 240, 360, and 480 mT at 36 kHz. Short arrows mark the feature at T_D . Insets: The dc magnetization transitions of each crystal in 0.2 mT.

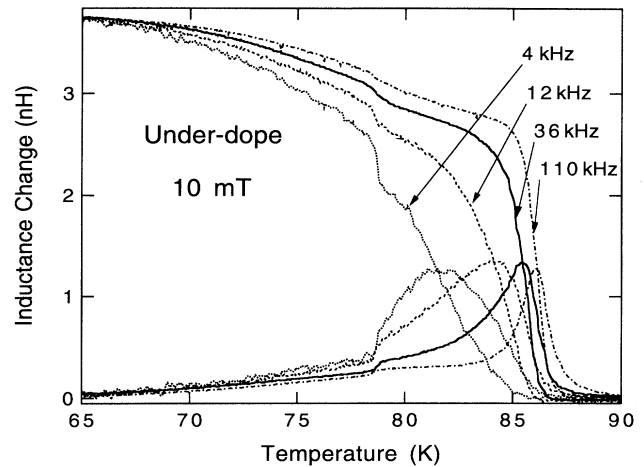


FIG. 4. Response of the underdoped crystal measured in 10 mT with various frequencies.

the c and ab directions, respectively). We assumed the mean-field temperature dependence for λ_{ab} in Eq. (1), and $\lambda_{ab}(0)$ is the penetration depth at zero temperature. It is interesting to note that most of the fluctuation theories predict essentially the same $B_D(T)$ except for the numerical factor. Because of the roughness of the theoretical estimations, the numerical factor should not be taken too seriously.

The solid lines in Fig. 5 are the fits of the data to Eq. (1); there are only two fitting parameters, the prefactor and T_c . The fit for the optimally doped crystal is excellent; the fit gives $T_c = 92.0$ K, which is consistent with the onset T_c , and the fitted prefactor is 82.8 [T K], which leads to $\gamma \approx 57$ if $\lambda_{ab}(0) = 180$ nm (Ref. 9) is assumed. Transport measurements done on the series of crystal prepared in the same way give the resistivity ratio ρ_c / ρ_a of 7×10^3 at 100 K for the optimum dope,¹⁴ which suggests $\gamma = 80$; therefore, the γ value obtained from the fit

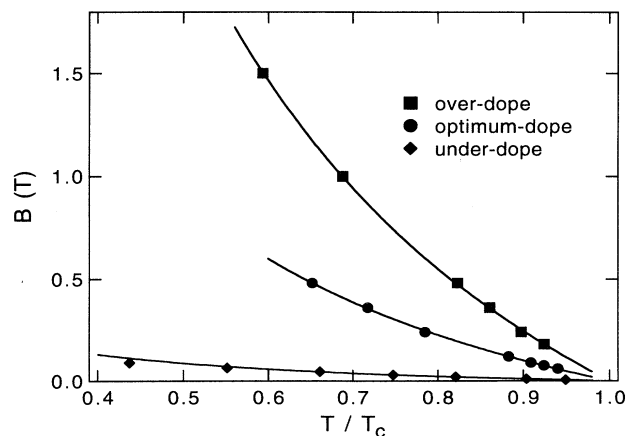


FIG. 5. $T_D(B)$ for the three crystals in the B - T phase diagram, where the temperature was normalized by each T_c . The solid lines are the fits to Eq. (1).

is quite reasonable, particularly if the roughness of the theoretical estimation is considered. The fit for the overdoped crystal is as good as that for the optimally doped crystal; the fit gives $T_c = 74.1$ K, which is consistent with the onset T_c to the accuracy of 1 K, together with the prefactor of 162.9 [T K]. For the underdoped crystal, the data above 55 K ($T/T_c > 0.6$) are fitted very well to Eq. (1); however, the data below 55 K start to deviate from the fitted curve. Such failure of the fit at low temperatures may be due to the presence of quantum fluctuations⁵ and/or the deviation from the mean-field temperature dependence in λ_{ab} . The fit shown in the figure gives $T_c = 87.7$ K, which again is consistent with the onset T_c to the accuracy of 1 K, and the prefactor of 7.54 [T K].

To understand the meaning of the above results, it should be noted that γ decreases with increasing doping,^{12,14} and at the same time $\lambda_{ab}(0)$ is expected to decrease because the carrier density is increased upon doping. Therefore, the prefactor in Eq. (1) should become larger with increasing doping. The results discussed above for the three crystals agree indeed with this expectation.²² Although the theories for the thermally induced dimensional crossover are rather diverse and not yet sophisticated, our result in Fig. 5 is quite impressive. The

good fits of $T_D(B)$ lines with the predicted dimensional crossover line and, more strikingly, its shift with the change in the anisotropy of the crystals, justify our attribution of the feature occurring at T_D to the thermally induced dimensional crossover.

In conclusion, we observed a step in the field-cooled linear ac-magnetic response measured with a miniature two-coil mutual inductance technique, in three $\text{Bi}_2\text{Sr}_2\text{CaCu}_2\text{O}_x$ single crystals with various doping states in magnetic fields parallel to the c axis. The step appeared at a frequency-independent temperature T_D . This feature can hardly be attributed to a second dissipation peak caused by vortex diffusion, but can possibly be understood as a consequence of the thermally induced dimensional crossover. The magnetic-field dependence of T_D agrees well with the theoretical prediction for the crossover line. Furthermore, the $T_D(B)$ line shifted to higher fields with increasing doping (decreasing anisotropy), which is consistent with the theoretical expectation.

We would like to thank R. Ikeda, L. N. Bulaevskii, E. H. Brandt, L. I. Glazman, D. A. Huse, P. L. Gammel, S. Akita, and H. Kubota for helpful discussions.

*Present address: AT&T Bell Laboratories, Murray Hill, NJ 07974.

¹L. I. Glazman and A. E. Koshelev, *Phys. Rev. B* **43**, 2835 (1991).

²L. L. Daemen *et al.*, *Phys. Rev. B* **47**, 11 291 (1993).

³M. C. Hellerqvist *et al.*, *Physica (Amsterdam) C* **230**, 170 (1994).

⁴J. R. Clem, *Phys. Rev. B* **43**, 7837 (1991).

⁵R. Ikeda, *J. Phys. Soc. Jpn.* **64**, 1683 (1995).

⁶D. G. Steel, W. R. White, and J. M. Graybeal, *Phys. Rev. Lett.* **71**, 161 (1993); W. R. White, A. Kapitulnik, and M. R. Beasley, *ibid.* **66**, 2826 (1991).

⁷J. H. Cho *et al.*, *Phys. Rev. B* **50**, 6493 (1994); Y. M. Wan, S. E. Hebboul, and J. C. Garland, *Phys. Rev. Lett.* **72**, 3867 (1994).

⁸R. Cubitt *et al.*, *Nature* **365**, 407 (1993).

⁹S. L. Lee *et al.*, *Phys. Rev. Lett.* **71**, 3862 (1993).

¹⁰A. Schilling *et al.*, *Phys. Rev. Lett.* **71**, 1899 (1993).

¹¹H. Pastoriza *et al.*, *Phys. Rev. Lett.* **72**, 2951 (1994).

¹²K. Kishio *et al.*, in *Critical Currents in Superconductors*, edited by H. W. Weber (World Scientific, Singapore, 1994), p.

339.

¹³M. V. Feigel'man, V. B. Geshkenbein, and A. I. Larkin, *Physica (Amsterdam) C* **167**, 177 (1990).

¹⁴Y. Kotaka *et al.*, *Physica (Amsterdam) C* **235-240**, 1529 (1994).

¹⁵A. T. Fiory *et al.*, *Appl. Phys. Lett.* **52**, 2165 (1988); B. Jeanerret *et al.*, *ibid.* **55**, 2336 (1989); A. Yazdani *et al.*, *Phys. Rev. Lett.* **70**, 505 (1993).

¹⁶Y. Ando *et al.*, *Phys. Rev. B* **50**, 9680 (1994).

¹⁷C. J. van der Beek and P. H. Kes, *Phys. Rev. B* **43**, 13 032 (1991).

¹⁸E. H. Brandt, *Physica (Amsterdam) C* **195**, 1 (1992).

¹⁹E. H. Brandt, *Phys. Rev. Lett.* **68**, 3769 (1992).

²⁰T. T. M. Palstra *et al.*, *Phys. Rev. B* **41**, 6621 (1990).

²¹A. Gupta *et al.*, *Phys. Rev. B* **48**, 6359 (1993).

²²Since $\lambda_{ab}(0)$ is not known for the overdoped and the underdoped, it is dangerous to derive γ for these two; if we dare to assume $\lambda_{ab}(0)$ to be 160 and 300 nm for the overdoped and underdoped, respectively, the fitted prefactors give γ of 45 and 112.